SCIENTIFIC COMMITTEE
THIRTEENTH REGULAR SESSION

Rarotonga, Cook Islands
9 – 17 August 2017

Prediction of shooting trajectory of tuna purse seine fishing

WCPFC-SC13-2017/EP-WP-03

Chun-Woo Lee[1], Jihoon Lee[2], Subong Park[3]

[1] Division of Marine Production System Management, Pukyong National University, Busan, Korea.

[2] Division of Marine Technology, Chonnam National University, Yeosu, Korea.

[3] Department of Fisheries Physics, Pukyong National University, Busan, Korea.

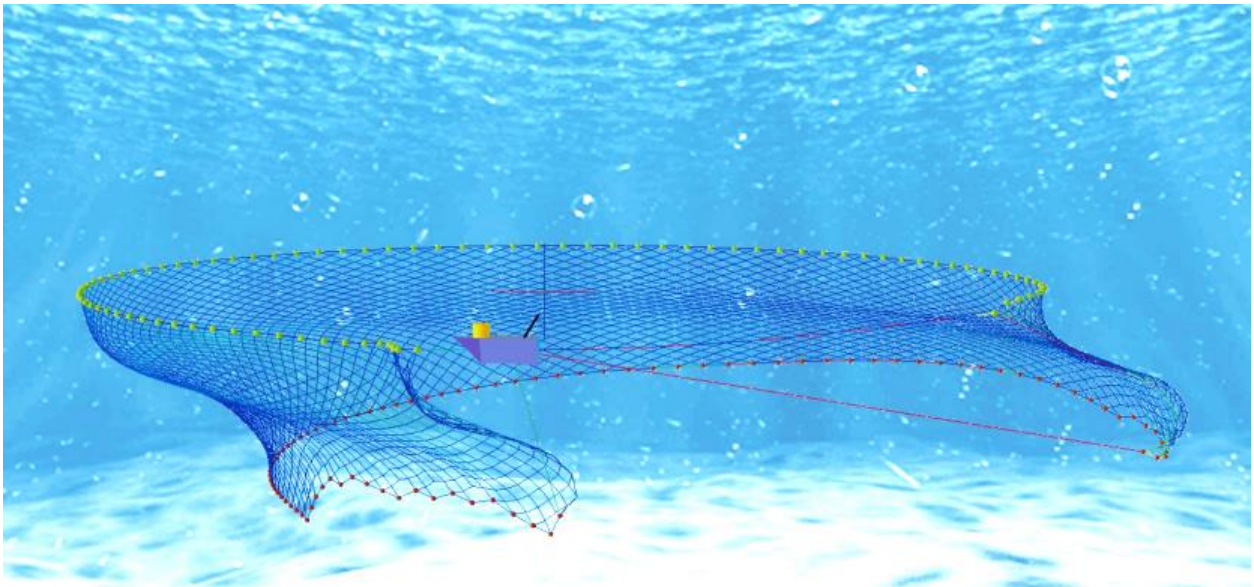

Prediction of shooting trajectory of tuna purse seine fishing

Authors:

Chun-Woo Lee*

Jihoon Lee

Subong Park

Division of Marine Production System Management,
Pukyong National University,
45 Yongso-ro, Busan 48513, Korea.
cwlee@pknu.ac.kr

This paper is submitted to the Fisheries Research and under review.

1. Introduction

Purse seines are used in areas of maximum fish concentration since they are more effective than other gear for catching pelagic fish. Thus, purse seining is one of the most efficient advanced fishing methods; because of the efficiency of this method, relatively few vessels are needed to harvest resources that are suitable for exploitation by purse seine methods (Ben-Yami, 1994). However, it is also complicated to deploy purse seines efficiently, as the deployment depends on the correct placement of the net relative to the fish school, as well as on the dominant environmental conditions.

Surface nets can, in principle, be used everywhere, in both marine and inland areas with sufficient space for the operation of a large net. A purse seine comprises large netting walls used to surround the aggregated fish both from the sides and from underneath, thus preventing them from escaping by diving downward. Apart from a few exceptions, purse seines are surface nets. Each netting wall is framed by a floatline at the top and a leadline at the bottom. The fish school reacts sensitively to the net during the operation. The school, or any other accumulation of fish on which the seine is set, may be stationary (mainly when attracted to light or to a fish aggregating device (FAD)) or mobile. In general, the fish schools captured by purse seining can be divided into unassociated schools and associated schools according to the fish school formation. The operation for unassociated schools is performed for fish schools at the surface and for schools that are feeding on baitfish. Meanwhile, the operation for associated schools is performed for log schools, FAD schools, and whale shark schools (Bromhead et al., 2003; Lee, 2016).

The Western & Central Pacific Fisheries Commission (WCPFC) limits FAD operation because of the bycatch problems with juvenile bigeye tuna and yellowfin tuna when FADs are operated in tuna purse seine fishery. FAD regulation is expected to be further strengthened in the future. Currently, the regulation for major purse seining countries in the Pacific Ocean offers two alternatives: in the first, FAD operation is forbidden from July to September and fishing operations are limited to 81 in total per year, whereas in the other, FAD operation is forbidden from July to October with no limitation on the total number of fishing operations per year. Furthermore, purse seine fishery is managed on FADs prohibition in WCPO according to the WCPFC Conservation of Management Measures (CMM) for 2014–2017 and to an additional measure for 2015/2016.

FAD operation has a high success rate in fishing because the targeted fish remain almost stationary. Meanwhile, the operation for unassociated fish schools has a higher failure rate because of errors in judgment regarding the fish school as well as unexpected fish behavior and inaccurate shooting trajectory prediction. The operation performed is selected by setting the shooting trajectory and initial shooting position, according to the accurate judgment and prediction of the fish school movement.

From a previous research (Lee, 2016) on the Korean purse seine fleet, a fishing operation is considered a failure if it is below 15 metric tons. The fishing success rate with FAD is 70%, whereas that for unassociated fish schools is 44%. The above fishing restriction affects Korean tuna purse seine fishery slightly, as Korea has a relatively low FAD operation ratio. However, it presents a significant obstacle to countries with relatively high FAD operation ratios. Therefore, the efficiency of fishing operations for unassociated fish schools must be improved by predicting the seine shooting trajectory through scientific calculation, considering the direction and speed of fish school movement. However, research on the calculation of the seine shooting trajectory is rare. Fridman (1973, 1986) attempted a theoretical calculation of the length of the purse seine considering the vessel speed and fish school speed.

This study proposes two purse seine shooting methods according to the speed of the target fish school. These shooting methods can be applied to both unassociated and associated fish schools. Shooting trajectories are presented according to specific scenarios, with example calculations shown. In addition, a shooting method based on the sinking depth of the leadline is presented. This method relies on determining the sinking depth of the leadline with elapsing time through numerical calculations or experiments.

2. Methods

2.1. Purse seine shooting method 1

When a school is moving from a point P_0 at a speed $\boldsymbol{V}_f$, the ideal shooting method causes the school to arrive at the center of the net, point $F_{0.5}$, when the shooting is complete. In actual fishing operations, after the net is shot, a tow line is attached at 20–30% of the net length; when the tow line is considered, the initial shooting position is point P_1. Here, it is better for the initial shooting point P_1 to be distant from the school as this minimizes the effect of the net on the behavior of the fish. Fig. 1 shows these parameters graphically. Assuming that the school maintains a constant speed and direction, we can obtain the gear length as follows described in the following sections.

The distance to be moved by the school, b, and the time, t, are given respectively by

$$b = 2R_g - \left(a + 2r_f\right) \tag{1}$$

$$t = \left(2R_g - \left(a + 2r_f\right)\right) / V_f \tag{2}$$

where R_g is the gear radius, a is the distance from the shooting circle to the school, r_f is the radius of the school, and V_f is the speed of the school.

The time taken for the ship to complete the shooting is

$$t = \mathrm{L} / V_s \tag{3}$$

where L is the gear length, which is the sum of the floatline length and the tow line length, and V_s is the speed of the ship.

Equations (2) and (3) should evaluate to the same time; therefore, given that $2R_g = \mathrm{L} / \pi$,

$$\left(\left(\mathrm{L} / \pi\right) - \left(a + 2r_f\right)\right) / V_f = \mathrm{L} / V_s \tag{4}$$

When the speed ratio $\mathrm{E} = (V_s / V_f)$ and the distance from the shooting circle to the school are given, the gear length (L) can be obtained by the following equation:

$$\mathrm{L} = \pi \mathrm{E}\left(\mathrm{a} + 2r_f\right) / \left(\mathrm{E} - \pi\right) \tag{5}$$

Here, the distance between the school and the shooting circle (a) can be calculated as follows:

$$\mathrm{a} = \left(\mathrm{E} - \pi\right)\mathrm{L} / \pi\mathrm{E} - 2r_f \tag{6}$$

In this case, there are two cases, depending on the difference between the speed ratio (E) and the value of π. That is, if E is larger than π, then (a) is positive. In this case, the fish school is placed inside the shooting circle. Conversely, if E is less than π, then (a) is negative. In this case, it means that the shooting will be performed when the fish school is placed outside the shooting circle. The gear will be shot out of the shooting circle. This is the case where the fish speed is fast.

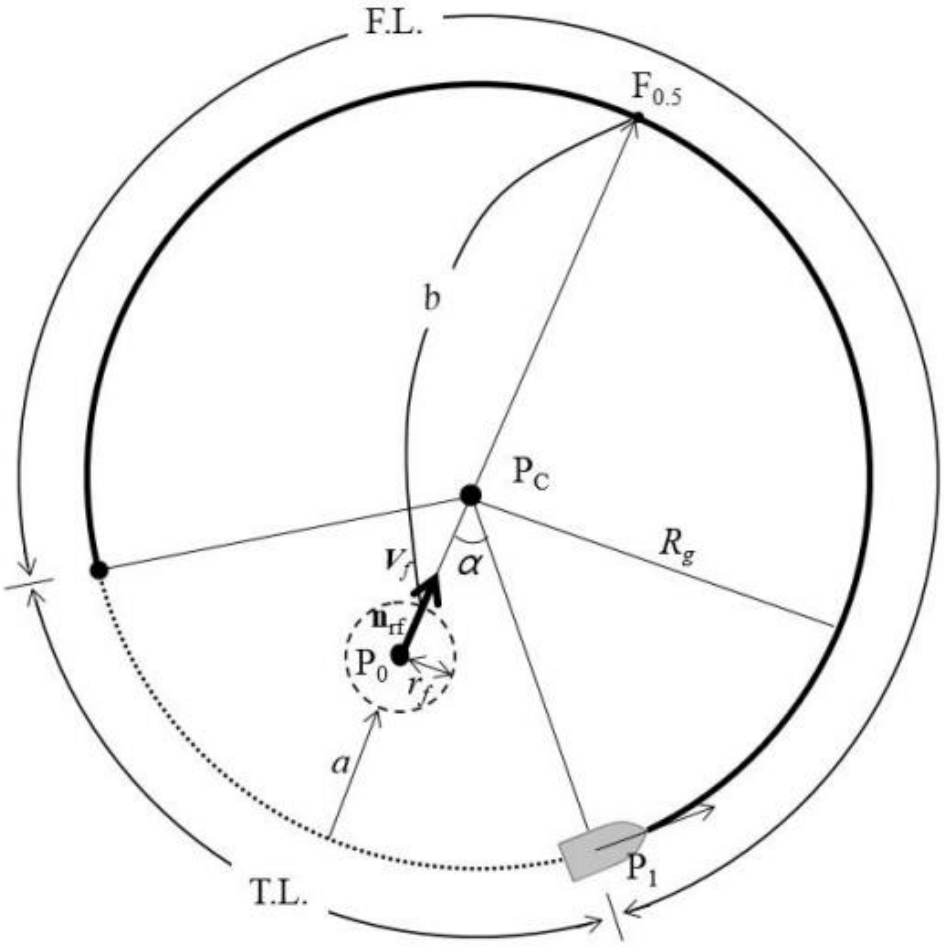

Fig. 1. Movement of fish school and shooting trajectory of purse seine shooting method 1 (F.L. : floatline length; T.L. : tow line length; R_g : gear radius; α : angle between the school direction and the line abeam of the ship; a : distance from the shooting circle to fish school; b : distance to be moved by the school; r_f : radius of the school; $\boldsymbol{V}_f$: speed vector of the school; $\mathbf{n}_{rf}$: unit vector of the school velocity; P_0 : position of the school; P_1 : initial shooting position; P_c : center of the shooting circle; $F_{0.5}$: center of the net).

2.2. Purse seine shooting method 2

This method is applicable to fast-swimming or stationary fish schools. On the assumption that the school swims at a constant velocity and direction, the school ideally arrives at the center of the shooting circle when the throwing is complete. Therefore, with the movement of the school accounted for, the initial shooting position is ahead of the school, with the school on the port side of the ship.

The first scenario (S1) is the conditions for the school to reach the center of the shooting circle when the shooting is 100% complete. The precise shooting position relative to the school is determined on the basis of the speed of the school, the seine shooting speed, and the length of the net. For example, in Fig. 2, if the school is swimming slowly, β can be smaller, but for fast-swimming schools, β must be large.

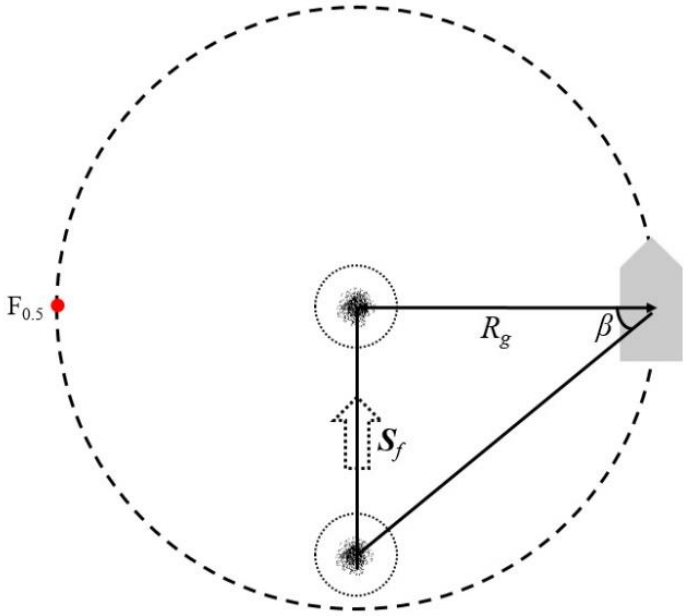

Fig. 2. Shooting trajectory of purse seine shooting method 2 ($F_{0.5}$: position where the shooting is 50% complete; R_g: gear radius; $\boldsymbol{S}_f$: distance moved by the school, β: angle between the initial position of the school and the line abeam of the ship).

In Fig. 2, β can be obtained by the following equation:

$$\beta = \tan^{-1}(\boldsymbol{S}_f / R_g) \tag{7}$$

Meanwhile, the distance to be moved by the school, $\boldsymbol{S}_f$, is given by

$$\boldsymbol{S}_f = \boldsymbol{V}_f \cdot t \tag{8}$$

where t is the time for the school and ship to move.

The time, t, of fish movement must be equal to the time used to complete the shooting of the seine, which is given by

$$t = \mathrm{L} / \boldsymbol{V}_s = 2\pi R_g / \boldsymbol{V}_s \tag{9}$$

Equations (7), (8), and (9) can be used to calculate the angle β. First, Equation (9) is substituted into Equation (8):

$$\boldsymbol{S}_f = \boldsymbol{V}_f \cdot (2\pi R_g / \boldsymbol{V}_s) = 2\pi R_g \cdot \left(\boldsymbol{V}_f / \boldsymbol{V}_s\right) = 2\pi R_g / E \tag{10}$$

Then, β can be estimated as follows:

$$\beta = \tan^{-1}(2\pi / E) \quad (11)$$

The second scenario (S2) is the conditions for the school to reach the center of the shooting circle when the shooting is 50% complete at the position $F_{0.5}$ in Fig. 2. In this case, a fast-swimming school can still be caught by shooting if the ship is located slightly ahead of the school; it remains possible to respond, to some extent, to changes in the swimming direction of the school. In this case, $L/2$ is substituted for L in Equation (9) and β is obtained by the method described above.

$$\beta = \tan^{-1}(\pi / E) \quad (12)$$

2.3. Deducing the shooting trajectory to account for the leadline depth

Although the two methods above can be used to predict the shooting trajectory, the leadline depth is entirely responsible for the ability of the net to block the path of the school arriving at point $F_{0.5}$ and $F_{0.3}$. Thus, the sink rate of the net is important in determining catch success. If experimental data or simulations were available for the seine sink rate, it would be possible to deduce a shooting trajectory that considers the ability to block the path of the school. Here, we aim to deduce the shooting trajectory on the basis of the leadline depth at the measurement points $M_{0.5}$ and $M_{0.3}$.

Fig. 3 shows the gear used to simulate the leadline depth in this study. The floatline length was 1860 m, which was consistent with the gear typically used on 1000 gross tonnage tuna purse seiners in Korea since 2013. The selected purse seine gear was mathematically modeled using a mass-spring model. The mathematical model used for the simulation was identical to that used in previous studies (Lee et al., 2008a, 2008b; Hosseini et al., 2011), and the calculation parameters were as follows: step size, 0.006 s; shooting speed, 12 kn.

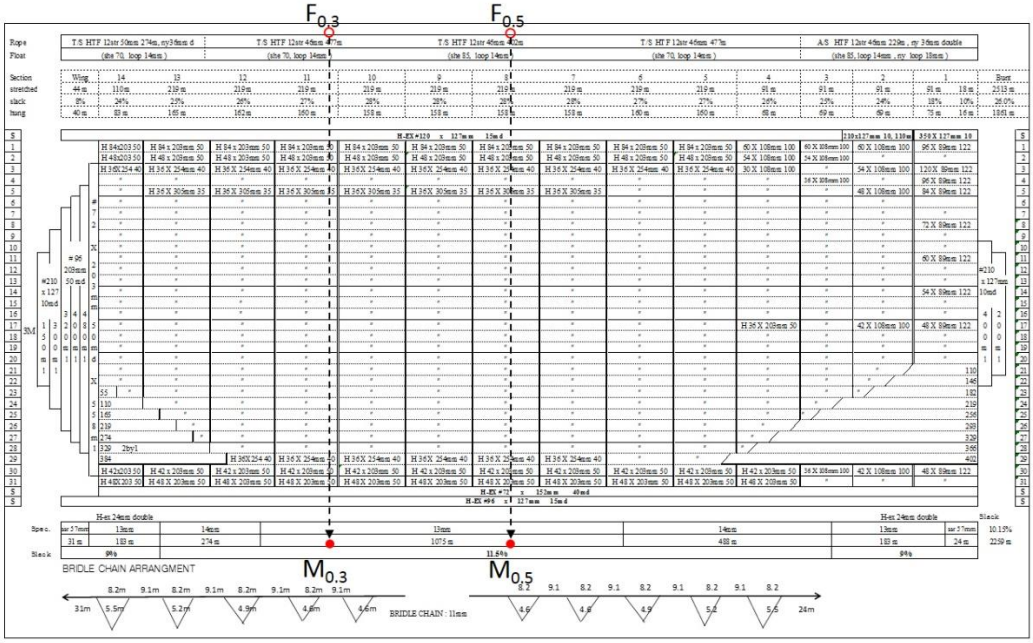

Fig. 3. 1,000 gross tonnages purse seiner gear ($F_{0.5}$: position where the length is 50% of the whole float line; $M_{0.5}$: measurement position at the leadline where the shooting is 50% complete; $F_{0.3}$: position where the length is 30% of the whole float line; $M_{0.3}$: measurement position at the leadline where the shooting is 30% complete).

3. Results

3.1. Computation examples

3.1.1. Calculation example for obtaining the initial shooting position P_1 by the method 1

Given a = 200 m, r_f = 50 m, $\boldsymbol{V}_f = \mathbf{i} + 2\mathbf{j}$ (m/s), and $\mathbf{P_0}(0,\ 0)$, $\mathbf{P_1}(x_1,\ y_1)$ can be obtained as follows, with a floatline length of 1860 m, tow line length of 600 m, and ship speed of 12 kn ($\boldsymbol{V}_s = 6$ m/s).

The unit vector of school velocity is given by the following equation:

$$\mathbf{n}_{\mathrm{rf}} = \frac{1}{\sqrt{5}}\mathbf{i} + \frac{2}{\sqrt{5}}\mathbf{j} \tag{13}$$

With the floatline length and the tow line length accounted for, α = 43.9°. From $2\pi R_g = \mathrm{L}$, $R_g = \mathrm{L}/2\pi = 2460/2\pi = 392$ (m). The distance from $\mathbf{P}_0$ to $\mathbf{P}_\mathrm{C}$ is $R_g - (a + 2r_f)$, which is equal to 92 m. By considering above unit vector, we can obtain the center position $\mathbf{P}_\mathrm{C}$ of shooting circle as follows:

$$x_\mathrm{C} = 41,\ y_\mathrm{C} = 82. \tag{14}$$

And the shooting circle and shooting start position can be obtained by taking into account for the float line and tow line length. Two points $\mathbf{P_1}(157.8,\ -292.2)$ and $\mathbf{P_{1-1}}(-328.4,\ -49.1)$ are obtained because of the symmetry around the line connecting $\mathbf{P}_0$ and $\mathbf{P}_\mathrm{C}$ (Fig. 4). These points are located at an angle of 43.9° on either side of the line. $\mathbf{P}_1$ is the initial shooting position for an anti-clockwise shot, whereas $\mathbf{P}_{1-1}$ is the initial shooting position for a clockwise shot. Since tuna purse seine fishing usually involves anti-clockwise shooting, this study focuses on the point $\mathbf{P}_1$.

On the other hand, if (a) is obtained from Equation (6) above when the speed ratio E is 3, 2.5, and 2, it is obtained as 63.0 m, -101.0 m, and -347.0 m, respectively. The shooting trajectory is shown in Fig. 5. As is apparent from the figure above, if the velocity ratio is less than 3.14, the value of (a) is negative and the shooting circle is created ahead of the fish school.

If the speed ratio is small, the shooting should start at a position far in advance of the fish school position and the fishing may fail to catch even if the direction or speed of the fish school is changed slightly. Moreover, when the shooting operation is started, the position of the skiff boat is located close to the course of the fish school, which is likely to affect the behavior of the fish school.

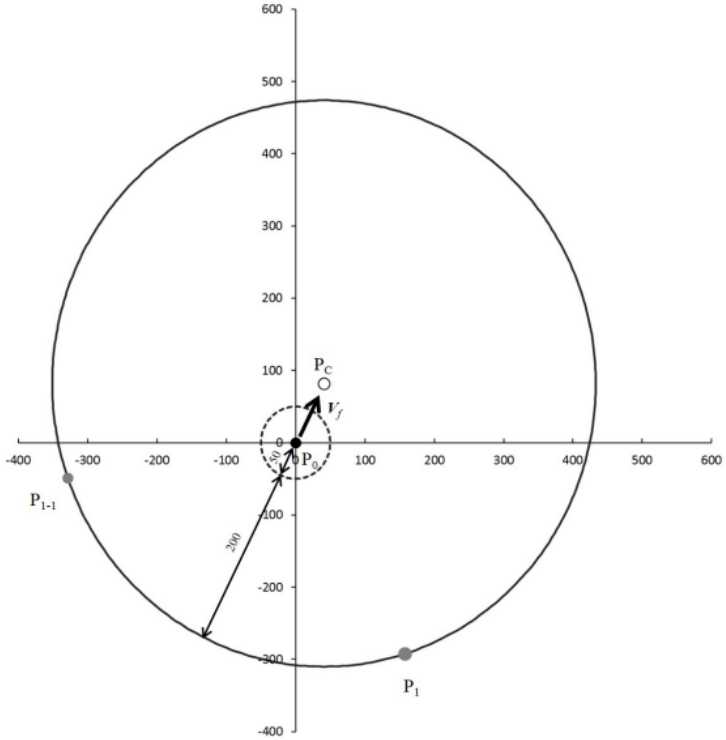

Fig. 4. The shooting circle and the initial shooting positions.

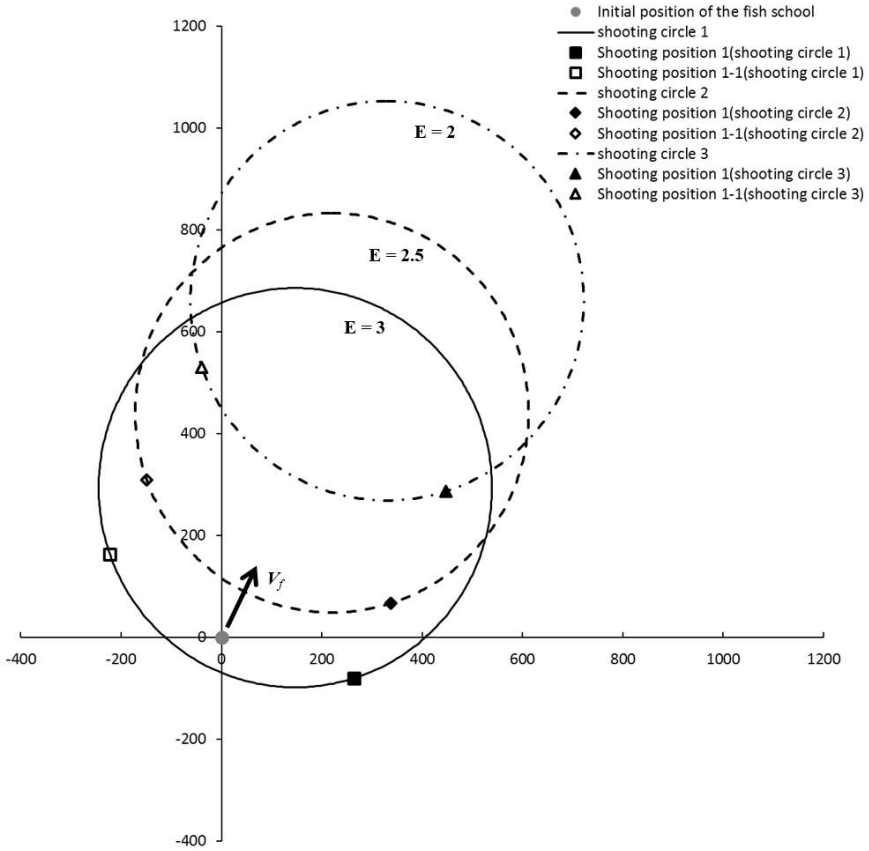

Fig. 5. Calculation of the initial shooting position with different speed ratio by the method 1.

3.1.2. Calculation example of the initial shooting position P_1 by the method 2

For the previous example, $\mathbf{P}_1(x_1,\ y_1)$ is obtained as follows using a condition perpendicular to the velocity vector of fish school.

$$x_1 = 350\,,\ y_1 = -175\,. \tag{15}$$

However, for a fast-swimming school, the initial shooting position must be ahead of the school, as shown in Fig. 6. Thus, the shooting position for each scenario can be calculated. Specifically, for a speed ratio of 3, the angle to the school, β, is calculated as in Table 1 and Fig. 7.

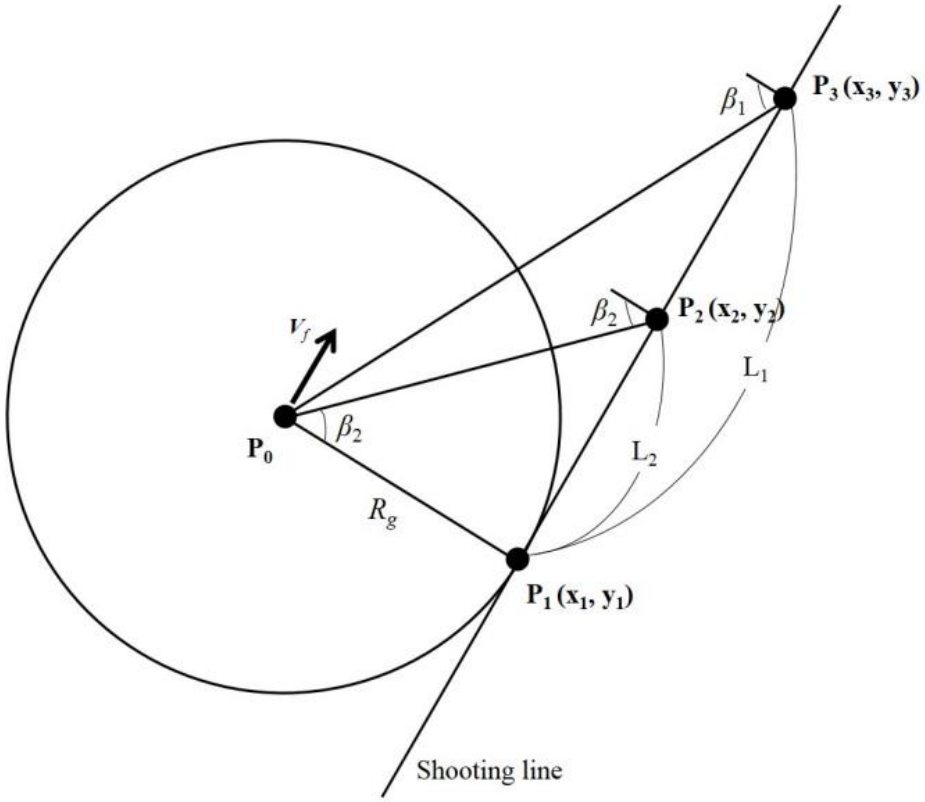

Fig. 6. Relationship between the initial shooting position and the angle to the school in each scenario.

Table 1. Angle to the school (β) and the length (L) for calculating the initial shooting position $\mathrm{P_1}$

Scenario	Angle to the school (β, °)	Length for calculating the initial shooting position (L, m)
$\mathrm{S_1}$	64.4 (β_1)	751 ($\mathrm{L_1}$)
$\mathrm{S_2}$	46.3 (β_2)	377 ($\mathrm{L_2}$)

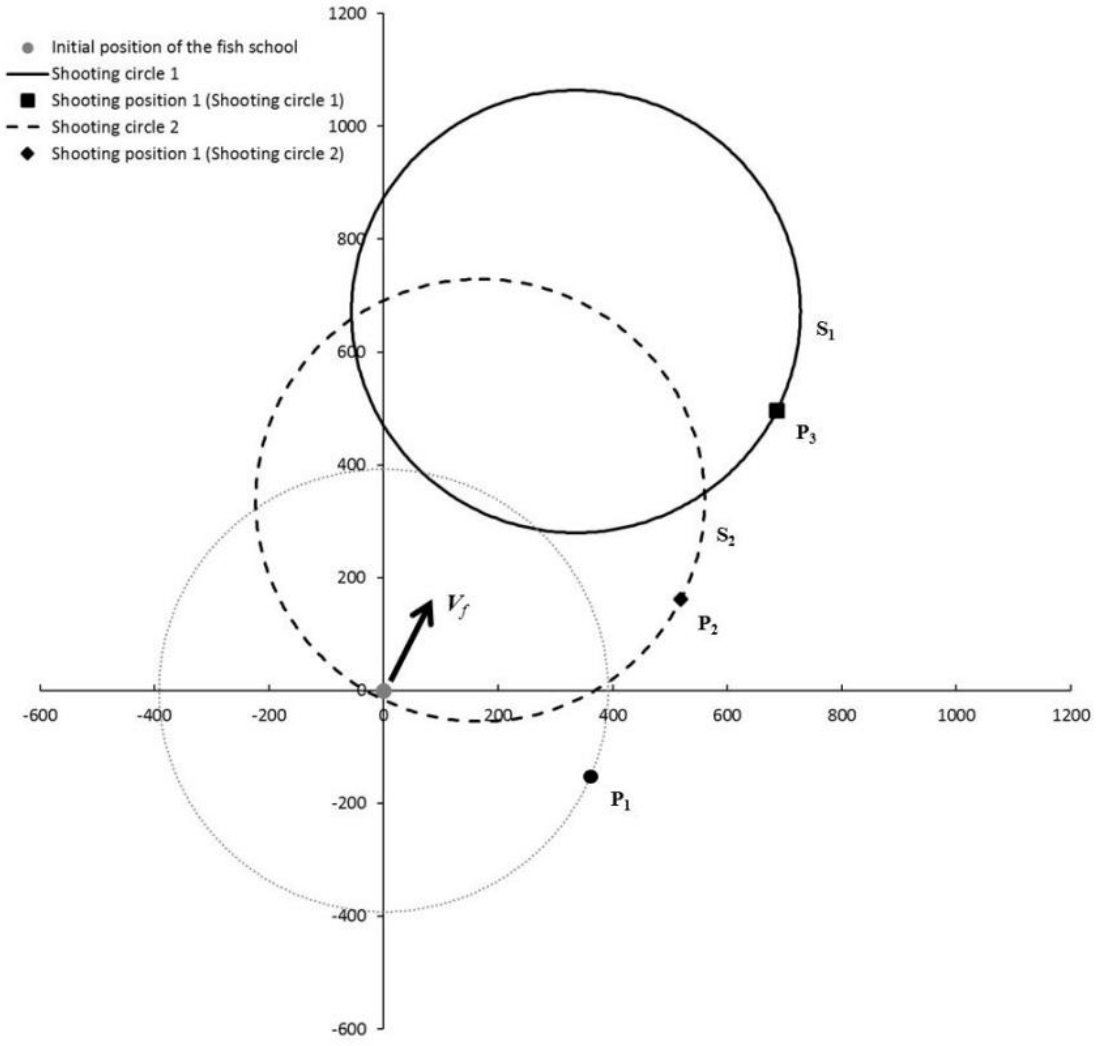

Fig. 7. Shooting trajectories for each scenario (S_1: scenario 1, S_2: scenario 2).

3.2. Simulation results of the gear behavior

The simulation conditions were equal to those in the examples given above, with a shooting speed of 12 kn, floatline length of 1860 m, and tow line length of 600 m. Fig. 8 shows the results of the simulation. This simulation not only deduced the three-dimensional behavior of the gear from the commencement of the shooting, but also provided more detailed data, such as the tension in each of the lines, the shape of the mesh, and the depth and sinking speed of each part of the gear. Fig. 9 shows the depth of the leadline at point $M_{0.3}$, $M_{0.5}$. The leadline depth increased over time, but the rate of increase gradually decreased. This is because the initial sinking speed was high, but the resistance of the net increased as it sank, thereby decreasing the sinking speed. This is consistent with the results of previous studies (Hosseini et al., 2011; Kim et al., 2007).

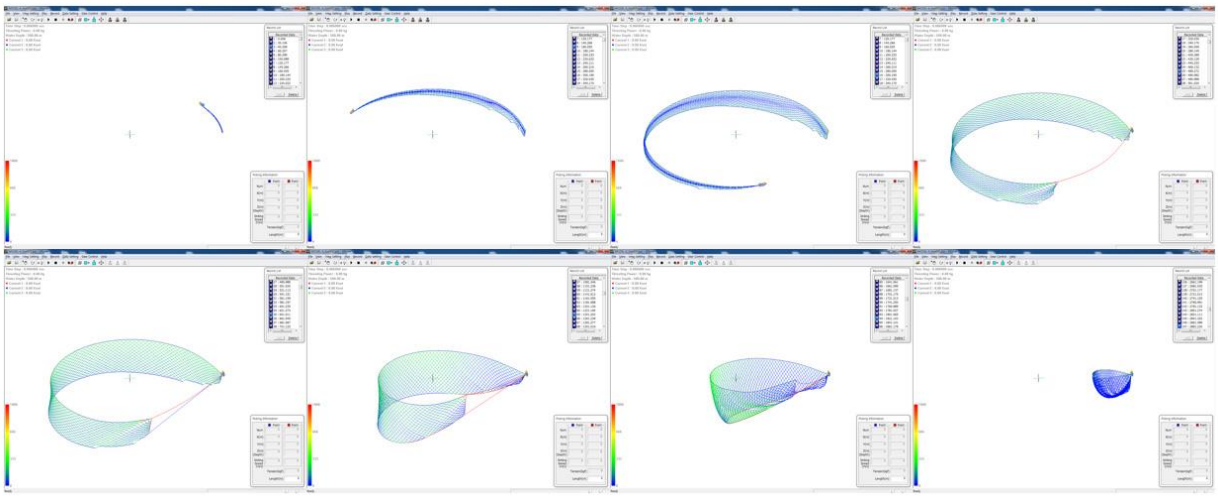

Fig. 8. Simulation results during the shooting and pursing operation.

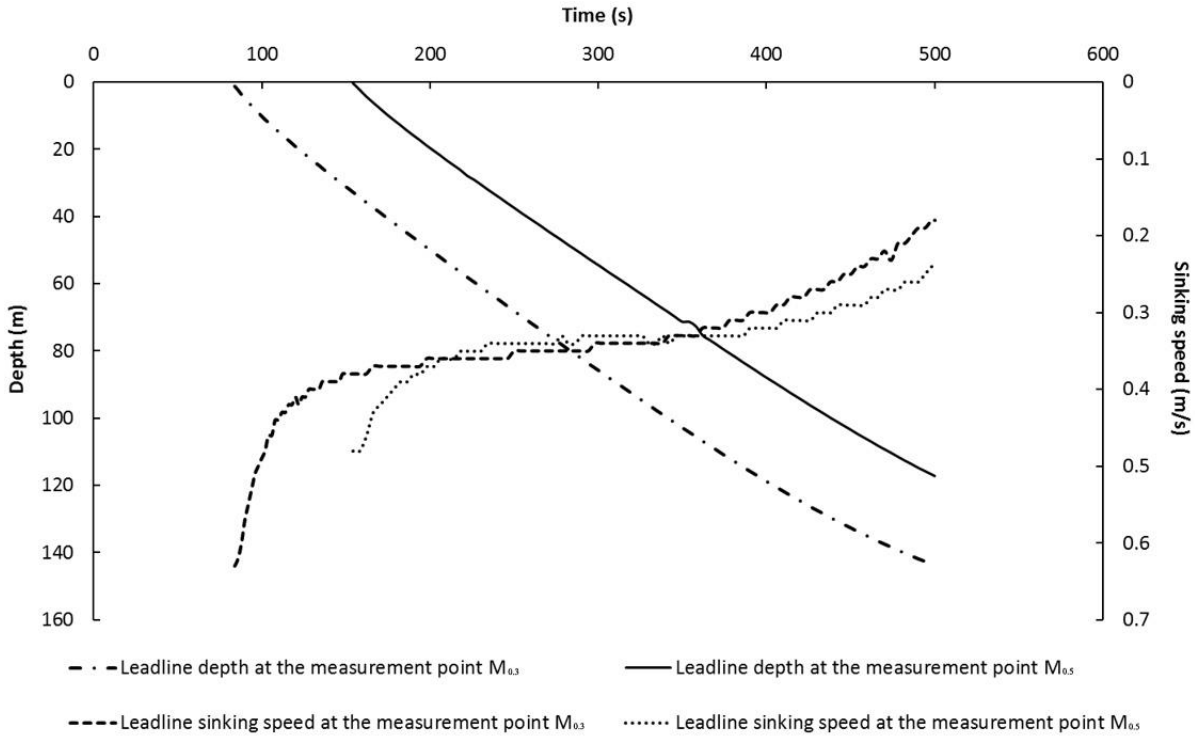

Fig. 9. Depth and sinking speed of the leadline at points $M_{0.3}$ and $M_{0.5}$.

3.3. Shooting trajectory according to the leadline depth

Through the above simulation, the depth of the sinker line of each part of the gear can be known over time, and, therefore, the shooting trajectory can be obtained on this basis. When the front tip of a fish school with a speed ratio of 4 arrived at a location on the $F_{0.5}$ - $M_{0.5}$ line of the net, the shooting trajectory of the shooting method 1 was obtained under the condition that the depth of the sinker line reached 50 m, 75 m, and 100 m, as presented in Fig. 10. Table 2 shows the relationship between the moving distance of the fish school and the depth of lead line while the speed ratio varies from 2 to 4.

When the front tip of a fish school with a speed ratio of 4 arrived at a position on the $F_{0.3}$ - $M_{0.3}$ line of the net, the shooting trajectory of shooting method 2 was obtained under the condition that the depth of the sinker line reached 50 m, 75 m, and 100 m, as shown in Fig. 11. Table 3 shows the relationship between the moving distance of the fish school and the depth of lead line while the speed ratio varies from 2 to 4.

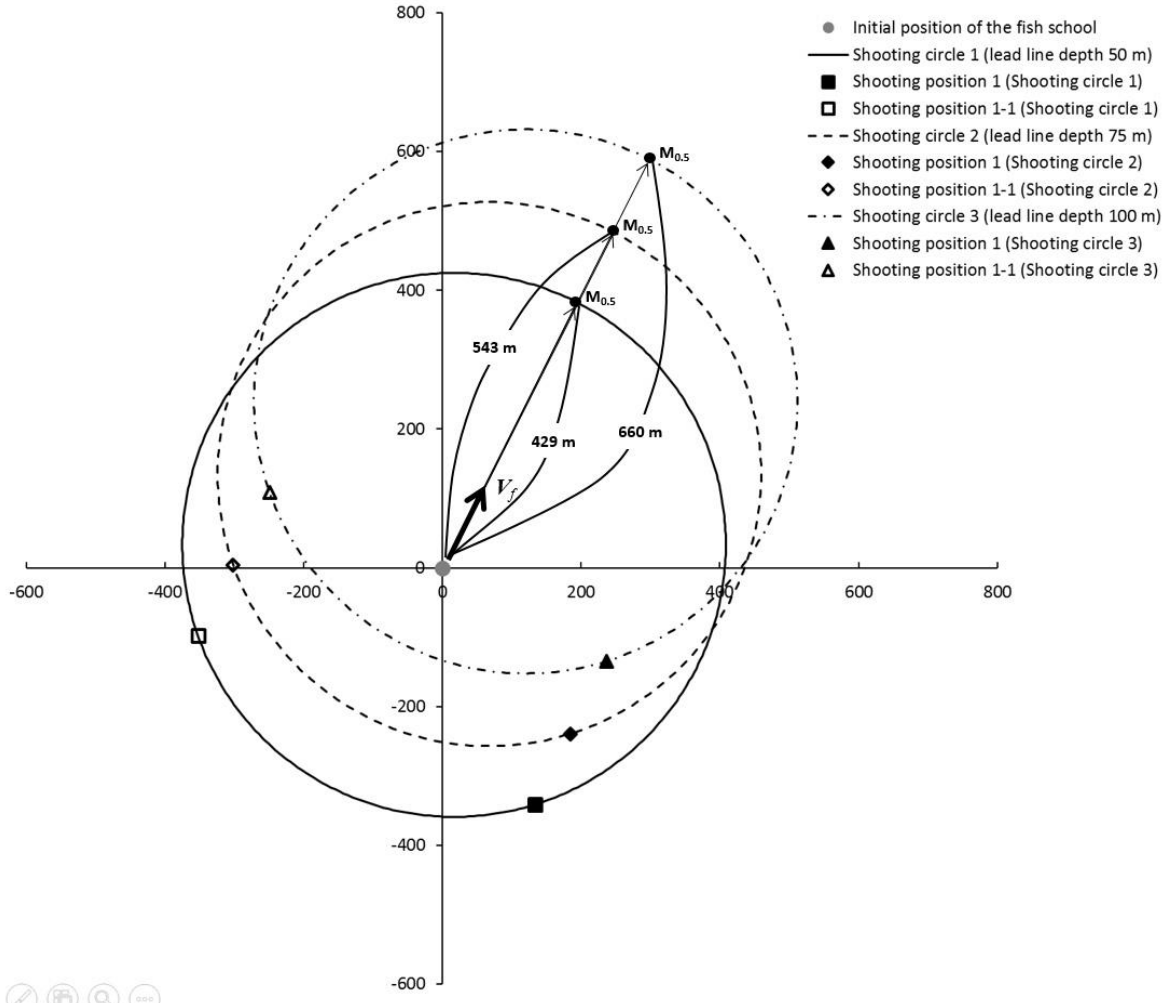

Fig. 10. Shooting trajectories by the method 1 for different leadline depths at a school speed of 1.5 m/s (circle 1: leadline depth, 50 m; circle 2: leadline depth, 75 m; circle 3: leadline depth, 100 m).

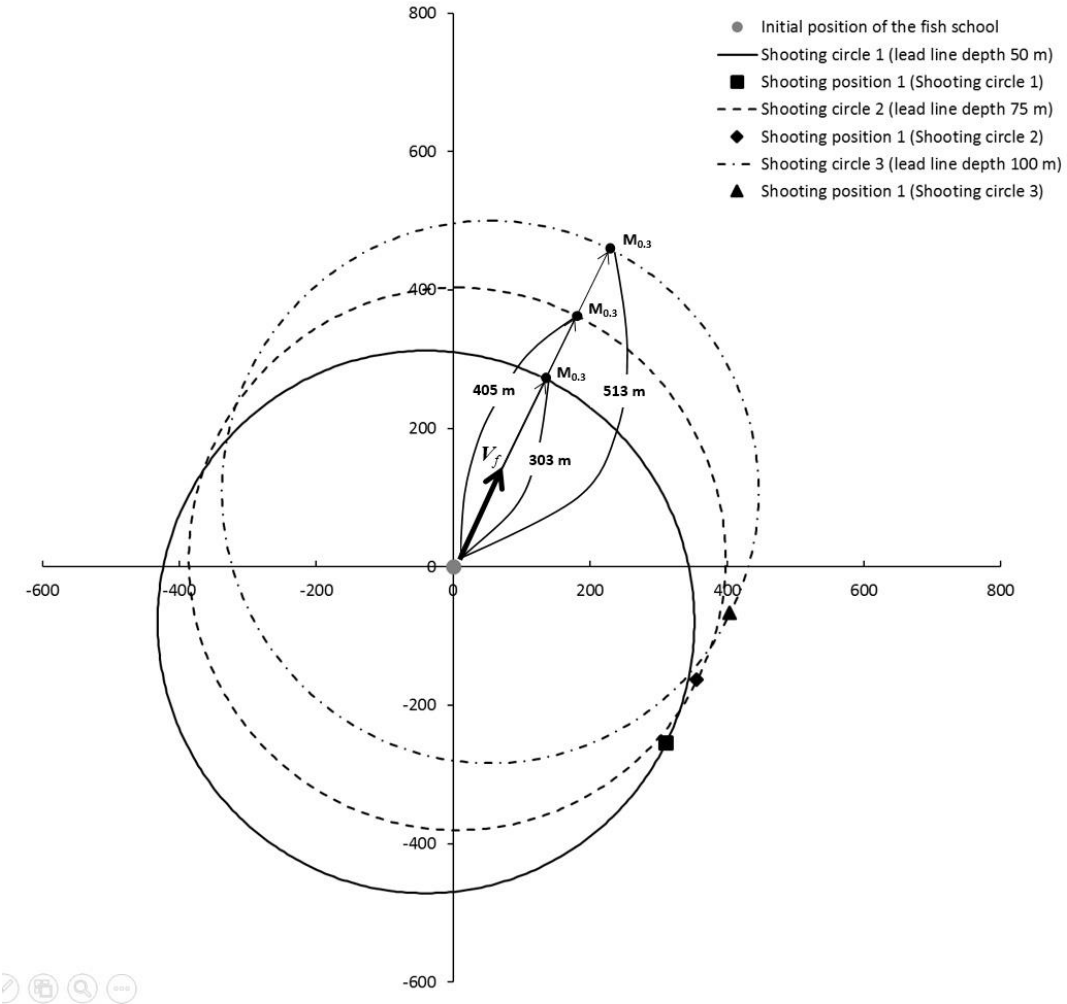

Fig. 11. Shooting trajectories by the method 2 for different leadline depths at a school speed of 1.5 m/s (circle 1: leadline depth, 50 m; circle 2: leadline depth, 75 m; circle 3: leadline depth, 100 m).

Table 2. Distance traveled by the school during the time for the leadline to sink to a given depth by the method 1

Speed ratio (E)	School speed (V_f , m/s)	Leadline depth ($M_{0.5}$, m)	Time elapsed (t , s)	Distance traveled by the school (S , m)
2.0	3	50	286	858
		75	362	1086
		100	440	1320
2.5	2.4	50	286	686
		75	362	869
		100	440	1056
3.0	2	50	286	572
		75	362	724
		100	440	880
3.5	1.7	50	286	486
		75	362	615
		100	440	748
4.0	1.5	50	286	429
		75	362	543
		100	440	660

Table 3. Distance traveled by the school during the time for the leadline to sink to a given depth by the method 2

Speed ratio (E)	School speed (V_f , m/s)	Leadline depth ($M_{0.5}$, m)	Time elapsed (t , s)	Distance traveled by the school (S , m)
2.0	3	50	202	606
		75	270	810
		100	342	1026
2.5	2.4	50	202	485
		75	270	648
		100	342	821
3.0	2	50	202	404
		75	270	540
		100	342	684
3.5	1.7	50	202	343
		75	270	459
		100	342	581
4.0	1.5	50	202	303
		75	270	405
		100	342	513

4. Discussion

The two shooting methods presented in this study each have advantages and disadvantages. Shooting method 1 is suited to slower-swimming schools, although approaching the school too closely may occur. Moreover, for fast-swimming schools, the shooting circle is located considerably ahead of the school, whereas the shooting is performed very near the path of the school, and, therefore, the risk of failure is high for even slight changes in the school direction. Conversely, in shooting method 2, the initial shooting position is farther from the school, meaning that it is less likely to stimulate school movement; the opportunity to respond to changes in the school movement direction is also larger. However, a successful catch becomes difficult if the fish become aware of the net at point $F_{0.3}$ and escape toward the initial shooting position $\mathbf{P}_1$; therefore, when a skiff boat is used to control the school's behavior, movement toward point $\mathbf{P}_1$ must be prevented.

When the depth of the gear is unpredictable, either shooting method 1 or 2 can be selected or an intermediate shooting method can be used. When the sinking speed of the gear can be analyzed or predicted experimentally, it is more appropriate to select the shooting circle with consideration of the leadline depth and school depth. As shown in the analysis above, the seine sinking speed is important in determining the blocking of the school's path. The mean weight per unit length of the gear in our simulation was 6.73 kg/m. Since the sinking speed of the gear varies according to the materials and composition of the gear, this analysis must be conducted for each individual seine. The sinking speed can be improved by increasing the weight per unit length; however, this also requires increased flotation, which, in turn, corresponds to a bulkier gear and a heavier fatigue load on the net; careful choices are therefore necessary to balance these effects. Other methods of increasing the sinking speed include increasing the mesh size, using knotless netting, or selecting high-density gear materials.

The shooting trajectory for each of the two shooting methods for varied tow line lengths is also considered. In shooting method 1, a longer tow line increases the distance between the initial shooting position and the school. This effect is similar for shooting method 2. As the tow line is lengthened, the school position moves further within the shooting circle. This indicates increased opportunity to respond to changes in school speed and direction during the shooting. Lengthening the tow line can be considered similar to enlarging the gear. However, care must be used because a longer tow line also means the gate through which the school can escape is wider during the pursing operation.

Since the school velocity vector can change at any time, once a school has been detected, the shooting circles presented above must be recalculated at every moment to accommodate the changes in the speed or direction of the school. Since this is difficult to achieve by manual calculations, it would be logical to use assisting software that could draw shooting circles using a computerized tool on the basis of the velocity vector of the school obtained by the sonar system.

5. Conclusion

Establishing fishing techniques for unassociated fish schools with high failure rates in tuna purse seine operations is an important international issue. Many countries are currently engaged in FAD-oriented operations, entailing many bycatches of non-target species. Solving these problems requires the application of fishing techniques with high success rates to unassociated fish schools. In this study, we have proposed shooting methods and shooting trajectory calculation methods for fishing of an unassociated fish school. These shooting methods can be selected depending on the speed and direction of the fish. In addition, for a known leadline sinking depth, or a depth monitored through analysis of the fishing gear, a shooting trajectory based on this depth is also suggested. The proposed methods for shooting trajectory prediction can contribute to international efforts to reduce bycatches of non-target species.

Acknowledgment

This research was a part of the project titled “Development of a large trawl system with low-carbon emission and improved stability during operation,” funded by the Ministry of Oceans and Fisheries, Korea.

References

Barkley, R.A., Neill, W.H., Gooding, R.M., 1978. Skipjack tuna, Katsuwonus pelamis, habitat based on temperature and oxygen requirements. Fish. Bull. 78(3), 653–662.

Ben-Yami, M., 1994. Purse seine manual. FAO, Fishing News Books. Wiley, Hoboken, NJ, pp. 406.

Bromhead, D., Foster, J., Attard, R., Findlay, J., Kalish, J., 2003. A review of the impact of fish aggregating devices (FADs) on tuna fisheries: Final report to the Fisheries Resources Research Fund. Bureau of Rural Science, Australia. pp. 121.

Fridman, A.L., 1973. Theory and design of commercial fishing gear, Israel Program for Scientific Translations, Jerusalem. pp. 489.

Fridman, A.L., 1986. Calculation for fishing gear designs, FAO fishing manual, Fish News Books Ltd., London, pp. 191–197.

Hosseini, S.Y., Lee, C.W., Kim, H.S., Lee, J., Lee, G.H., 2011. The sinking performance of the tuna purse seine gear with large-meshed panels using numerical method. Fish Sci. 77, 503–520.

Kim, H.Y., Lee, C.W., Shin, J.K., Kim, H.S., Cha, B.J., Lee, G.H., 2007. Dynamic simulation of the behavior of purse seine gear and sea-trial verification. Fisheries Research. 88, 109-119.

Lee, C.W., Kim, Y.B., Lee, G.H., Choe, M.Y., Lee, M.K., Koo, K.Y., 2008a. Dynamic simulation of a fish cage system subjected to currents and waves. Ocean Eng. 35, 1521–1532.

Lee, J.H., Karlsen L., Lee C.W., 2008b. A method for improving the dynamic simulation efficiency of underwater flexible structures by implementing non-active points in modelling. ICES J. Mar. Sci. 65(9), 1552–1558.

Lee, M.K., 2016. Study on fishing characteristics and strategies of Korean tuna purse seine fishery in the Western and Central Pacific Ocean. PhD Thesis. Pukyong National University, Busan, Korea. pp. 161

Orúe, B., Lopez, J., Moreno, G., Santiago, J., Soto, M., Murua, H., 2016. Fishers’ echo-sounder buoys to estimate biomass of fish species associated with fish aggregating devices in the Indian Ocean. IOTC-2016-WPTT18-28.

Senina, I., Lehodey, P., Calmettesa, B., Nicol, S., Caillot, S., Hampton, J., Williams, P., 2016. Predicting skipjack tuna dynamics and effects of climate change using SEAPODYM with fishing and tagging data. WCPFC-SC12-2016/EB WP-01, 1-70.